

Chitosan/Alginate/Diatom을 이용한 조직공학용 다공성 세포지지체 연구

Yusuf Özcan[†], Dicle Erden Gönenmiş, Esranur Kızıllhan, and Cem Gök*

Department of Biomedical Engineering, Pamukkale University

*Department of Metallurgical and Material Engineering, Pamukkale University

(2021년 1월 7일 접수, 2022년 3월 17일 수정, 2022년 4월 25일 채택)

Highly Porous Biocomposite Scaffolds Fabricated by Chitosan/Alginate/Diatom for Tissue Engineering

Yusuf Özcan[†], Dicle Erden Gönenmiş, Esranur Kızıllhan, and Cem Gök*

Department of Biomedical Engineering, Pamukkale University, 20070, Denizli, Turkey

*Department of Metallurgical and Material Engineering, Pamukkale University, 20070, Denizli, Turkey

(Received January 7, 2021; Revised March 17, 2022; Accepted April 25, 2022)

Abstract: Tissue scaffolds based composite material have attracted great attention in the field of bone tissue engineering. Therefore, researchers are looking for new materials to be used for composite tissue scaffolding. We aimed to produce the effect of high porous and non-toxic scaffolds as hydrogels with two different contents using chitosan, alginate and diatom. Beads were made from alginate and alginate/diatom hydrogels and additionally coated in dilute chitosan solution. Obtained alginate-chitosan (AC) and alginate/diatom-chitosan (ADC) beads were lyophilized. High-porous AC scaffold and both high-porous and nano-porous ADC scaffold were examined in terms of density, porosity, swelling tests and morphologic, chemical, cytotoxic analysis. In this study, high porosity with approximately 450 μm pore size was found for AC and ADC scaffolds. The average pore size of diatom in ADC was acquired as 280 nm. Moreover, AC and ADC did not show any cytotoxic effects on HEK293 cells. Our results clearly indicated that scaffolds have an alternative potential in the field of tissue engineering.

Keywords: biocomposite, diatom, chitosan, alginate, scaffold, tissue engineering.

Introduction

Recently, scientific studies and advances in the field of tissue engineering have led to an increased interest in the development of components in the structure of scaffold. In the light of these developments, the purpose of tissue engineering is to carry out restoration and regeneration studies of damaged tissues and organs.¹ Therefore, tissue engineering studies have become an alternative field for the formation of tissue scaffolds. The building blocks of tissues in our body are the cells that make up the basic units. These cells cluster together to form the extracellular matrix (ECM). As a result, scaffold is expected to be of a biodegradable high porous structure. Also, it must have strong mechanical properties that allow cells to

structure, promote cell growth and differentiation, and most importantly, to be biocompatible.²⁻⁴ Tissue engineering creates scaffolds that simulate ECM, providing a natural environment for cell viability, growth, and proliferation. The difference in tissue scaffolds depends on the hydrogels obtained with different physical and biological properties. Tissue engineering methods have gained an important place in the last decade to produce tissue scaffolds. These methods are the most preferred production technologies such as freeze-drying, electrospinning, gas foaming, phase separation.⁵⁻⁷ The freeze-drying technique is based on the sublimation of a portion of the ice at a low temperature of the mixture. This method makes it easy to produce different biomaterials with different pores. The success of the created three-dimensional tissue scaffolds depends on the stages of production and the concentration of the produced hydrogels.⁸

Polymers and their derivatives have been investigated and used in many fields since 1990. Because polymers and their

[†]To whom correspondence should be addressed.
ozcan@pau.edu.tr, ORCID[®]0000-0003-4355-5383
©2022 The Polymer Society of Korea. All rights reserved.

derivatives have environmentally friendly structures and practical applications in biomedical, pharmaceutical and cosmetic fields from micro to nanoscale engineering.^{9,10} Thus, Hydrogel, which is the natural three-dimensional structure of tissue scaffolds, has many unique properties such as high porosity, biodegradability, biocompatibility, high water holding capacity without scaffold dissolution and similar physical properties of natural tissues. This allows it to simulate the natural extracellular matrix.¹¹⁻¹⁴ Hydrogels can be obtained in the form of polymers in two ways: synthetic and natural. Among natural hydrogels, materials such as alginate and chitosan are very good natural polymers for tissue engineering applications. Alginate is a naturally occurring polysaccharide derived from brown plankton.¹⁵⁻¹⁷ Alginate has the structures of 1,4-linked β -D-mannuronic acid and 1,4- α -L-guluronic acid and is a hydrogel formed by repeating these structures.¹⁸ Particularly scaffolds in tissue engineering has many advantages, including high hydrophilicity, biodegradability, biocompatibility, ease of crosslinking, and high mechanical properties.¹⁹⁻²¹ Alginate can cross-link between divalent cations (*e.g.*, Ca^{2+} , Sr^{2+} , and Ba^{2+}) and a functional group such as carboxyl through ionic interactions. The crosslinks perform alginate insoluble in an aqueous solution and culture medium. This helps scaffold structures to remain supportive in the form of hydrogels.^{20,22,23}

Chitosan is a polysaccharide derived from (1-4)-2-amino-2-deoxy- β -D-glucan.²³ It is also obtained from the most plentiful chitin in nature. Chitin is found in the exoskeletons and shells of insects, as well as in the cell walls of fungi.²⁴ Chitosan does not dissolve at high pH. However, chitosan has hemostatic, bacteriostatic, anticarcinogenic, and fungistatic biological properties. These properties make it biocompatible and biodegradable.²⁵ As mentioned earlier, both chitosan and alginate are naturally occurring polysaccharides. Therefore, chitosan as a molecule has hydroxyl and amino groups, while alginate has carboxyl groups that give chitosan a negative charge.^{26,27} When used alone, chitosan acts as an extracellular adhesive. For this reason, chitosan cannot adhere to scaffold and cannot survive. Since alginate is negatively charged, they are suitable biomaterials for cell seeding. Alginate can bind positively charged chitosan due to their negative charge; therefore, it provides a stronger bond between cells.²⁷

Diatoms are natural silica materials that form protective structures in scaffolds in the form of unicellular eukaryotic photosynthetic microalgae. Diatoms have microscopically well-spaced pores on the inner and outer surfaces. These porous structures have a high specific surface area, high

adsorption, and low density.²⁸ Furthermore, due to low cost and high availability by its nature, it allows it to be used as a reinforcing filler, abrasive, insulating material, membrane, and cell. Diatom also has high bioactivity.^{29,30}

In this study, we aimed to obtain a three-dimensional tissue scaffold with high swelling, good mechanical strength, high biodegradability and porous structure characteristics from their production by forming a bio-composite material in the form of hydrogel from natural materials as chitosan-diatom-alginate.

Experimental

Materials. Alginic acid sodium salt was purchased from Sigma-Aldrich (USA). Chitosan (medium molecular weight) was obtained from Sigma-Aldrich (Iceland). Acetic acid (Glacial, 100% Anhydrous) was purchased from ISOLAB chemicals (Wertheim, Germany). Diatomaceous earth (suitable for most filtrations) was purchased from Sigma-Aldrich (USA). Anhydrous calcium chloride (CaCl_2) was bought from Merck (Czech Republic). Ethyl alcohol, 99.9%, was purchased from ISOLAB Chemicals (Wertheim, Germany). MTT (3-(4,5-dimethylthiazol-2-yl)-2,5-diphenyl-2H-tetrazolium bromide) and Dulbecco's modified Eagle medium (DMEM) were purchased from Sigma-Aldrich (USA). All of these chemicals were of analytical grade. Distilled water was used throughout this work.

Preparations of Chitosan/Alginate and Chitosan/Alginate/Diatom Beads Scaffolds. Sodium alginate was dissolved in distilled water at a concentration of 5% (w/v) to prepare chitosan/alginate beads scaffolds. Then chitosan was prepared at a concentration of 0.3% in 0.1% acetic acid. The resulting alginate solution was added dropwise to prepared 1 M CaCl_2 solution using a Pasteur pipette (3 mL).

For the preparation of beads of chitosan/alginate/diatom scaffolds, sodium alginate was dissolved in distilled water at a concentration of 5% (w/v) and chitosan was prepared at a concentration of 0.3% in 0.1% acetic acid as the same procedure preparation of chitosan/alginate beads. Then, 0.1 g of diatom was added to 20 mL of alginate solution and the mixture was allowed to mix until being homogeneous. The resulting mixture of diatom alginate was dropped into a prepared 1 M CaCl_2 solution using a Pasteur pipette (3 mL).

AC and ADC beads were created with the same method, solidified in 1 M CaCl_2 for 20 minutes and then removed, then washed with distilled water and filtered. These balls were added to the stirred chitosan solution at a constant stirring rate

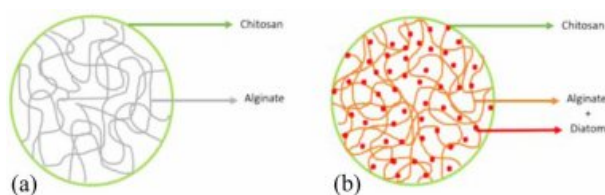


Figure 1. (a) AC beads; (b) ADC beads.

at room temperature and stirred for 30 minutes. The resulting chitosan coated beads were filtered by a filter paper (Figure 1).

Experimental conditions such as the distance between CaCl_2 solution and dropping point, the number of drops in the gelling medium, and the temperature per minute have been systematically optimized. The resulting balls were spherical with a smooth surface. Samples AC and ADC were stored at -20°C overnight. The stored samples were subjected to a lyophilization process.

Density, Porosity and Swelling. The density of prepared AC was calculated from the apparent texture density of the ADC scaffold (ρ_{scaffold}), dry weight, and the volume of these scaffolds:

$$\text{Density } d = m/v = \rho_{\text{scaffold}} \quad (1)$$

The porosity of scaffolds was determined according to the equation below:

$$\text{Porosity } \% = (\rho_{\text{real}} - \rho_{\text{scaffold}}) / \rho_{\text{real}} \times 100 \quad (2)$$

Where the pores of lyophilized structures ρ_{skeletal} filled with ethyl alcohol, ρ_{real} is calculated.

The water absorption (swelling) of the porous tissue base was determined using the following equation:

$$\text{Swelling } \% = (W_w - W_d) / W_d \times 100 \quad (3)$$

Where W_w and W_d are wet and first dry pier weight, respectively.

Scanning Electron Microscopy with Energy Dispersive Spectroscopy. Chitosan coated alginate and alginate/diatom composite scaffolds were analyzed by scanning electron microscopy (SEM)³¹ for investigated pore size, morphology and dispersion of diatom rigid and porous cell walls in chitosan and alginate structure. Before the analysis, beads were coated with a palladium/gold sheet under argon gas by a coating device. After this, SEM analysis was made with Zeiss Supra 40VP (Germany). The average pore size of the beads and the diatoms within the beads were measured utilizing SEM images. Chemical elements on the material surface were

detected with energy dispersive spectroscopy (EDS) (Zeiss Supra 40VP, Germany).

Fourier Transform-Infrared Spectroscopy. Fourier transform-infrared spectroscopy (FTIR) (Thermo Scientific Nicolet iS50, Germany) was used to characterize the interactions between the components in scaffolds prepared at intermolecular level. In addition, the functional groups and chemical bonds of AC and ADC beads scaffolds were examined at a resolution of 0.5 cm^{-1} and frequency of $400\text{-}4000\text{ cm}^{-1}$ using a Thermo Scientific Nicolet iS50 model FTIR.³²

Cytotoxicity. 3-(4,5-Dimethylthiazol-2-yl)-2,5-diphenyl-tetrazolium bromide (MTT) assay (BioVision, USA) was used to determine *in vitro* cytotoxicity of scaffolds on the HEK293 cell line. The extraction of scaffolds was performed as described in³³ with slight modifications. Briefly, scaffolds weighing 4.7 mg were extracted in 20 mL DMEM at 37°C for 24 h in the orbital shaker. After 24 h, medium was removed and filtered. An equal amount of medium without extract was added to untreated cells (control). The cells (1.5×10^3 cells/well) were incubated in 96-well plates at 37°C overnight. After the incubation, cells were exposed to a medium in which scaffolds were kept at different concentrations (5, 10, 25, 50, and 100 μL) for another 24 h. Then, the medium was removed and 10 μL of MTT reagent (in 100 μL medium) was added to each well and incubated for 4 h in the same conditions. Afterwards, MTT was removed carefully and 50 μL of DMSO (dimethyl sulfoxide) was added to each well. The absorbance was measured at 590 nm using Epoch Microplate Spectrophotometer (BioTek, USA) and averaged and the viability curves were drawn up.

Then, the cell vitality % was identified according to the formula below. Furthermore, control samples were also examined (cells were incubated without bead scaffolds):

$$\text{Cell vitality } \% = \frac{\text{Sample absorbance}}{\text{Control absorbance}} \times 100 \quad (4)$$

Statistical Analysis. All experiments were run in duplicates. Data were provided as means, including standard error of means (SEM). A Student's t-test was used to compare the data, and $p < 0.05$ was chosen for statistical significance.

Results and Discussion

Physical Properties of AC and ADC Scaffolds. The structure and size of porosity in scaffold has an important role. Like porosity, density and swelling behavior of the structure

Table 1. Density, Porosity, Swelling of Freeze-dried AC and ADC Tissue Scaffolds

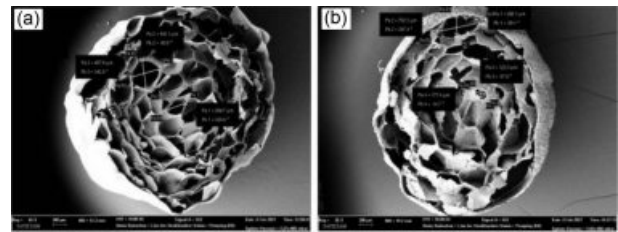
	Density (g/cm ³)	Porosity (%)	Swelling (%)
AC	0.193±0.002	36.3±0.1	81.2±0.5
ADC	0.207±0.002	58.3±0.1	81.8±0.5

are also significant.³⁴ Table 1 summarizes the density, porosity and swelling of freeze-dried AC and ADC scaffolds. The density of AC and ADC beads was calculated as 0.193 g/cm³ and 0.207 g/cm³, respectively. The reason for the increase in density in ADC is due to the diatom in the structure. The porosity of the ADC is higher than AC beads as seen in Table 1. Hence, we can see that diatoms increase the porosity of the structure. Considering the results on the table, it is seen that the swelling degrees were almost the same. Although the porosity increased, a change in degrees of swelling of AC and ADC beads were not observed.

This study was carried out to investigate whether a porous skeleton structure can be obtained by doping diatoms to the structure. According to our results, there are no large-scale studies of scaffolding containing diatoms for tissue engineering applications. It provides good biocompatibility with a variety of hydrogels and can be considered suitable for the use in tissue engineering because of its biodegradability. When the literature studies on tissue engineering applications are examined, there are some studies on biopolymeric materials such as chitosan and alginate. In these studies, different tissues were evaluated by various techniques. For example, Li and co-workers studied chitosan-alginate hybrid scaffolds for bone tissue engineering.³⁵ In this study, chitosan and alginate solution were lyophilized in a freeze dryer, but we used diatoms with nanopores. Thus, in addition to the micropores in the structure, nanopores are provided.

A high degree of porosity is important in tissue engineering as it allows cells to migrate to scaffold and settle in it. It increases the applicability of scaffolds thanks to the appropriate swelling degree and density, sufficient porosity, enhanced protein adsorption, and increased mineralization effects. Tissue scaffolds similar to AC have been seen in the literature, and their physiological characteristics were found to be consistent with previous studies.^{35,36} It has been seen that the porosity value that comes with diatom doping in ADC increases considerably compared to AC. Here it is seen that ADC is more applicable in tissue scaffolds.

SEM/EDS Analysis. SEM images of AC and ADC scaffold

**Figure 2.** SEM images of (a) AC; (b) ADC (scaffold with the porosity measure).

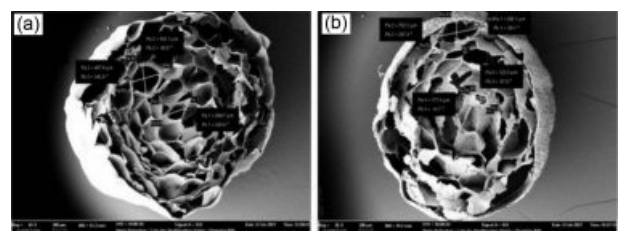
displays that nano-porous and highly-porous microstructure were obtained by freeze-drying methods. Interconnected open pores have been seen in AC and ADC scaffolds with a pore size of approximately in a range of 299–457 μm and 122–703 μm, respectively (Figure 2). The results obtained show that scaffolds are porous and of the desired size. Therefore, both scaffolds are suitable for cell attachment and new bone tissue growth.³⁵ Also, AC scaffold is well defined and interconnected pore structure,³⁶ the addition of diatoms to AC composite resulted in a reduction of the pore size.

SEM images of AC and ADC complex beads showed highly porous structures. Average pore sizes were identified by using cross-section images of AC and ADC scaffolds. When compared to AC scaffold, nanopore morphology was also formed in ADC with the presence of diatoms. It was seen that the morphology and pore size were influenced by diatom grains concentration and its dispersion grade in ADC scaffold (Figure 3).

The presence of diatom within ADC also created the nanopore size compared to AC scaffold. The average pore size of diatom within ADC was acquired to be in the range of 260–330 nm (Figure 4).

EDS spectra of composite AC and ADC scaffolds were presented in Figure 5. Due to the production method, the internal and external structures of the beads are made of different materials, so separate EDS spectra are given for both internal and external structures.

The external structure of ADC beads contains oxygen, car-

**Figure 3.** SEM images of (a) the diatom-containing ADC scaffold; (b) diatom dispersed in the ADC scaffold.

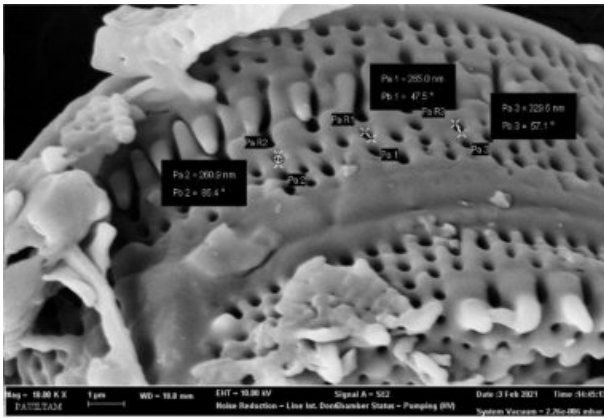


Figure 4. SEM image of diatom in ADC scaffold with the porosity measure.

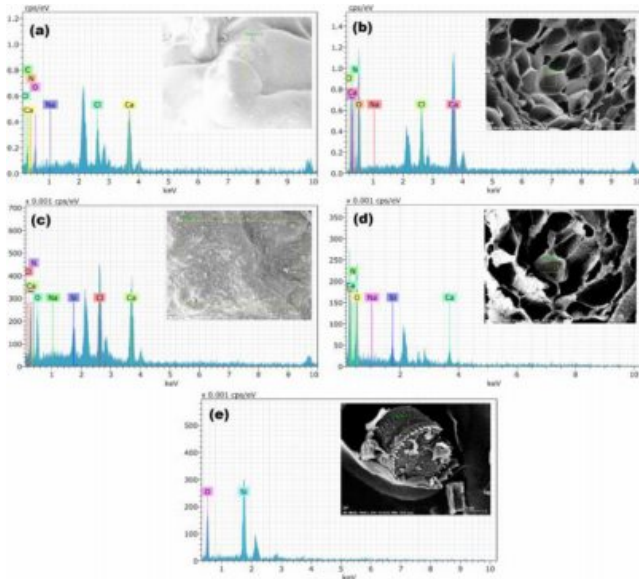


Figure 5. EDS spectrum of the external and internal structure of (a, b) AC; (c, d) ADC scaffold. EDS spectrum of (e) the diatom dispersed in ADC scaffold.

bon, calcium, nitrogen, chlorine and sodium elements as we expected. The element with the highest atomic rate in this structure was found to be oxygen with 39.66%. Afterwards, carbon and nitrogen elements were determined as 35.11% and 13.09%, respectively. The same elements were found in the EDS examination of the internal of AC structure. However, it was observed that the oxygen and carbon ratios increased to 51.54% and 40.09%, respectively, and the other element's ratios decreased. Similar elemental ratios in AC structure were also found in ADC beads. Besides, silicon element originating from diatom has been detected in the external and internal structure of ADC scaffold. As seen in Figure 5(e), only silicon

and oxygen elements were found in the structure in the EDS analysis of diatoms.

Although the optimum pore size for bone tissue engineering remains uncertain, researches attempting to determine the optimum pore size for this field has shown that pore sizes ranging from 80 to 500 μm are appropriate.³⁶ According to the results of our study, it is seen that our structure is in the optimum pore range. It also allows scaffolds at these pore sizes to allow for proliferation, cell adhesion, as well as a nutrient source to ensure proper bone tissue growth. A bone tissue was obtained by freeze-drying by adding fucoidan to the chitosan and alginate matrix structure by Venkatesan and co-workers.³⁶ It was observed that this composite structure increased bioactivity. In our study, the advantageous structure was obtained in bone tissue applications with porous structure characteristics by doping diatom to chitosan and alginate matrix. In these points, our materials are very suitable for tissue engineering applications and our results also supported this phenomenon.

FTIR Analysis. Alginate and chitosan are two different materials that have electrostatic attraction among themselves. According to literatures, FTIR spectra of alginate and diatom were discussed and then AC and ADC scaffolds were compared. FTIR spectra of AC and ADC scaffolds are given in Figure 6.

Tensile vibrations of alginate O-H bonds showed up in the range of 3000-3600 cm^{-1} . Tensile vibrations of the aliphatic C-H can be seen at 2920-2850 cm^{-1} . The bands observed at 1649 and 1460 cm^{-1} were interpreted to the asymmetric and symmetric tensile vibrations of the carboxylate salt ion. The subsequent bands are crucial for the characterization of derivatives and components of the alginate structure. The bands at 1107 and 935 cm^{-1} were interpreted to the C-O stretching vibration of the pyranosyl ring.³⁷

Tensile vibrations of chitosan were observed at 3478.68 cm^{-1} for O-H and 2924.13 cm^{-1} for C-H. The peaks at 1656.88 cm^{-1} , 1571.05 cm^{-1} , 1422.53 cm^{-1} , 1378.16 cm^{-1} , respectively, were

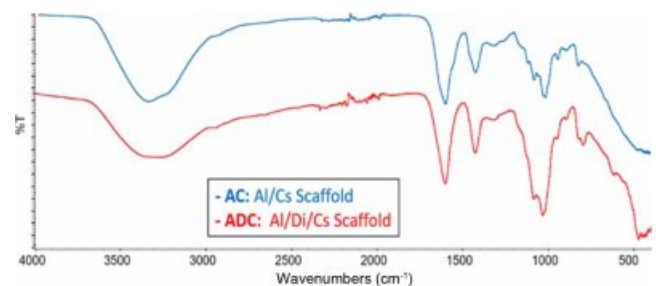


Figure 6. FTIR spectra of AC and ADC scaffolds.

associated with the entity of the C=O tensiling of amide I band, bending vibrations of the N-H, C-H bending, OH bending. The peak at 1157.31 cm^{-1} was stated for anti-symmetric tensiling of (C-O-C) bridge, 1075.33 cm^{-1} and 1025.18 cm^{-1} were estimated to the skeletal vibration including C-O tensiling.³⁸

The FTIR spectra obviously displays the characteristic peaks of diatom frustule, which involves Si-O-Si bending at 689 and 810 cm^{-1} , Si-O-Si tensiling at 947 cm^{-1} , and O-H tensiling of surface-bound hydroxyl groups at 3361 cm^{-1} , which would involve bound Si-O-H and water.³⁹ The characteristic peaks for carboxyl C-H tensiling at 2885 cm^{-1} (CH_2) and 2972 cm^{-1} (CH_3). This is owing to the remaining organic materials still clenched to the frustules even after acid digestion.⁴⁰

The single bond NH_2 group of chitosan interacts with the single bond COOH group of alginate. Therefore, a shift in amide and amino groups in chitosan is expected. Moreover, Bands at 1651 cm^{-1} and 1324 cm^{-1} had to be replaced with a new band at 1313 cm^{-1} due to the cross-linking of CaCl_2 and the interaction of the two single bonded COOH groups attached to the adjacent chains. The diatom displayed its characteristic peak at 1077 cm^{-1} Si-O single connection Si bond symmetric vibration.⁴¹ The 1593 cm^{-1} to 1417 cm^{-1} bands in ADC scaffold represent a possible interaction between the carbonyl group in chitosan and Si single bond OH group diatom.

Molecular chemical interactions between chitosan, alginate and diatom were investigated by FTIR. FTIR spectra were used to confirm the functional groups and interactions of scaffolds. The results are consistent with the previous studies. The IR results showed that the hybrid structure consisting of the components in the structure is miscible due to the strong electrostatic force and intermolecular hydrogen bonding. We can also say that the diatom was successfully conjugated to chitosan-alginate scaffolds from these results.^{35,42,43}

Cytotoxicity Determination. The cytotoxicity of scaffolds

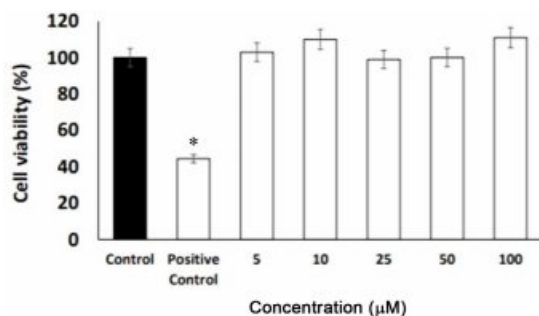


Figure 7. Effect of AC on HEK293 cells viability analyzed by MTT assay. Cells were treated for 24 h with the increased concentration of AC. Positive control: cisplatin ($50\text{ }\mu\text{M}$) ($*p<0.05$).

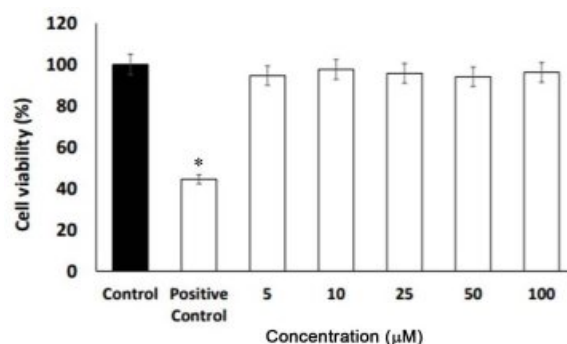


Figure 8. Effect of ADC on HEK293 cells viability analyzed by MTT assay. Cells were treated for 24 h with the increased concentration of ADC. Positive control: cisplatin ($50\text{ }\mu\text{M}$) ($*p<0.05$).

was determined as described in the material methods part by using the HEK293 cell line. As shown in Figure 7 and 8, the viability of cells was not changed significantly because of AC and ADC treatment. However, small decreases that were observed in different doses were not found to be statistically significant. It is well established that a small decrease in viability can be considered as a safe application of these materials for different purposes.

Conclusions

In this study, novel bio-nanocomposite is a promising material for the field of bone tissue engineering. It was prepared by using alginate, chitosan and diatom, which can be used as a bone tissue scaffold in tissue engineering. AC and ADC beads were prepared using the strong ionic interaction of the carboxyl groups of alginate and amino groups of chitosan. Additionally, diatom has been added to this composite structure to increase bioactivity. 3D-porous structure architecture demonstrated the advantages of ADC over AC scaffolds. As seen in SEM-EDS analysis, it is understood that the diatom containing ADC scaffold has nano-porous structures compared to the AC scaffold. As a result of the cytotoxicity studies performed at different rates, AC and ADC scaffold structures did not show any toxic effects. The controlled biodegradability, non-toxicity and improved apatite accumulation of ADC scaffold obtained with micro and nano structures may be useful for bone tissue engineering studies. The prepared material has the intended properties as a bone tissue. In this respect, it makes an important contribution to the literature and has a vital role in tissue engineering and biomedical application. Therefore, prepared material has shown its great potential in tissue engineering and biomedical sciences with its features. However, further tests

such as *in vivo* animal studies will be required to test this hypothesis.

Acknowledgments: The authors would like to thank the Scientific Research Council of Pamukkale University, Turkey, for research grant 2021FEBE011. The authors thanks to Molecular Biochemistry Laboratory of Biology Department of Pamukkale University for providing device usage and supports.

Conflict of Interest: The authors declare that there is no conflict of interest.

References

- Di silvio, L. 15-Bone tissue Engineering and Biomineralization. In *Tissue Engineering Using Ceramics and Polymers*; Boccaccini, A. R., Gough, J. E., Eds.; Woodhead Publishing: Cambridge, 2007; pp 319-331.
- Peter, S. J.; Miller, M. J.; Yasko, A. W.; Yaszemski, M. J.; Mikos, A. G. Polymer Concepts in Tissue Engineering. *J. Biomed. Mater. Res.* **1998**, 43, 422-427.
- Freed, L. E.; Vunjak-Novakovic, G.; Biron, R. J.; Eagles, D. B.; Lesnoy, D. C.; Barlow, S. K.; Langer, R. Biodegradable Polymer Scaffolds for Tissue Engineering. *Nat. Biotechnol.* **1994**, 12, 689-693.
- Kim, B. S.; Mooney, D. J. Development of Biocompatible Synthetic Extracellular Matrices for Tissue Engineering. *Trends Biotechnol.* **1998**, 16, 224-230.
- Yu, Y.; Hua, S.; Yang, M.; Fu, Z.; Teng, S.; Niu, K.; Zhao, Q.; Yi, C. Fabrication and Characterization of Electrospinning/3D Printing Bone Tissue Engineering Scaffold. *RSC Adv.* **2016**, 6, 110557-110565.
- Nie, W.; Peng, C.; Zhou, X.; Chen, L.; Wang, W.; Zhang, Y.; Ma, P. X.; He, C. Three-dimensional Porous Scaffold by Self-assembly of Reduced Graphene Oxide and Nano-hydroxyapatite Composites for Bone Tissue Engineering. *Carbon* **2017**, 116, 325-337.
- Costantini, M.; Barbetta, A. 6-Gas foaming technologies for 3D scaffold engineering. In *Functional 3D Tissue Engineering Scaffolds: Materials, Technologies, and Applications*; Deng, Y., Kuiper, J.B.T., Eds.; Woodhead Publishing: Cambridge, 2018; pp 127-149.
- Farhangdoust, S.; Zamanian, A.; Yasaei, M.; Khorami, M. The Effect of Processing Parameters and Solid Concentration on the Mechanical and Microstructural Properties of Freeze-casted Macroporous Hydroxyapatite Scaffolds. *Mater. Sci. Eng. C* **2013**, 33, 453-460.
- Özcan, Y.; İde, S.; Jeng, U.; Büttin, V.; Lai, Y. H. C.; Su, H. Micellization Behavior of Tertiary Amine-methacrylate-based Block Copolymers Characterized by Small-angle X-ray Scattering and Dynamic Light Scattering. *Mater. Chem. Phys.* **2013**, 138, 559-564.
- Özcan, Y.; Orujalipoor, I.; Huang, Y. C.; Büttin, V.; Jeng, U. S. Self-assembled and Nanostructured Copolymer Aggregations of the Tertiary Amine Methacrylate Based Triblock Copolymers. *Anal. Lett.* **2015**, 48, 2693-2707.
- Chai, Q.; Jiao, Y.; Yu, X. Hydrogels for Biomedical Applications: Their Characteristics and the Mechanisms Behind Them. *Gels* **2017**, 3, 6.
- Kopeček, J. Hydrogel Biomaterials: a Smart Future. *Biomaterials* **2007**, 28, 5185-5192.
- Peppas, N. A.; Bures, P.; Leobandung, W.; Ichikawa, H. Hydrogels in Pharmaceutical Formulations. *Eur. J. Pharm. Biopharm.* **2000**, 50, 27-46.
- Kamoun, E. A.; Omer, A. M.; Abu-Serie, M. M.; Khattab, S. N.; Ahmed, H. M.; Elbardan, A. A. Photopolymerized PVA-g-GMA Hydrogels for Biomedical Applications: Factors Affecting Hydrogel Formation and Bioevaluation Tests. *Arab. J. Sci. Eng.* **2018**, 43, 3565-3575.
- Rowley, J. A.; Madlambayan, G.; Mooney, D. J. Alginate Hydrogels as Synthetic Extracellular Matrix Materials. *Biomaterials* **1999**, 20, 45-53.
- Tonnesen, H. H.; Karlsen, J. Alginate in Drug Delivery Systems. *Drug Dev. Ind. Pharm.* **2002**, 28, 621-630.
- Joki, T.; Machluf, M.; Atala, A.; Zhu, J.; Seyfried, N. T.; Dunn, I. F.; Abe, T.; Carroll, R. S.; Black, M. P. Continuous Release of Endostatin from Microencapsulated Engineered Cells for Tumor Therapy. *Nat. Biotechnol.* **2001**, 19, 35-39.
- Yang, J. S.; Xie, Y. J.; He, W. Research Progress on Chemical Modification of Alginate: A Review. *Carbohydr. Polym.* **2011**, 84, 33-39.
- Fan, L.; Zhang, J.; Wang, A. In situ Generation of Sodium Alginate/Hydroxyapatite/Halloysite Nanotubes Nanocomposite Hydrogel Beads as Drug-controlled Release Matrices. *J. Mater. Chem. B* **2013**, 1, 6261-6270.
- Kuo, C. K.; Ma, P. X. Ionically Crosslinked Alginate Hydrogels as Scaffolds for Tissue Engineering: Part 1. Structure, Gelation Rate and Mechanical Properties. *Biomaterials* **2001**, 22, 511-521.
- Srinivasan, S.; Jayasree, R.; Chennazhi, K. P.; Nair, S. V.; Jayakumar, R. Biocompatible Alginate/Nano Bioactive Glass Ceramic Composite Scaffolds for Periodontal Tissue Regeneration. *Carbohydr. Polym.* **2012**, 87, 274-283.
- Tonnesen, H. H.; Karlsen, J. Alginate in Drug Delivery Systems. *Drug Dev. Ind. Pharm.* **2002**, 28, 621-630.
- Augst, A. D.; Kong, H. J.; Mooney, D. J. Alginate Hydrogels as Biomaterials. *Macromol. Biosci.* **2006**, 6, 623-633.
- Xu, J.; Ma, L.; Liu, Y.; Xu, F.; Nie, J.; Ma, G. Design and Characterization of Antitumor Drug Paclitaxel-loaded Chitosan Nanoparticles by W/O Emulsions. *Int. J. Biol. Macromol.* **2012**, 50, 438-443.
- Niaz, T.; Nasir, H.; Shabbir, S.; Rehman, A.; Imran, M. Polyionic Hybrid Nano-engineered Systems Comprising Alginate and Chitosan for Antihypertensive Therapeutics. *Int. J. Biol. Macromol.*

- 2016, 91, 180-187.
26. Ivanova, E. P.; Bazaka, K.; Crawford, R. 2-Natural Polymer Biomaterials: Advanced Applications. In *New Functional Biomaterials for Medicine and Healthcare*; Woodhead Publishing: New Delhi, 2014; pp 32-70.
 27. Kumbhar, S. G.; Pawar, S. H. Synthesis and Characterization of Chitosan-alginate Scaffolds for Seeding Human Umbilical Cord Derived Mesenchymal Stem Cells. *Biomed. Mater. Eng.* **2016**, 27, 561-575.
 28. Şan, O.; Gören, R.; Özgür, C. Purification of Diatomite Powder by Acid Leaching for Use in Fabrication of Porous Ceramics. *Int. J. Miner. Process.* **2009**, 93, 6-10.
 29. Wang, Y.; Cai, J.; Jiang, Y.; Jiang, X.; Zhang, D. Preparation of Biosilica Structures from Frustules of Diatoms and Their Applications: Current State and Perspectives. *Appl. Microbiol. Biotechnol.* **2013**, 97, 453-460.
 30. Gordon, R.; Losic, D.; Tiffany, M. A.; Nagy, S. S.; Sterrenburg, F. A. The Glass Menagerie: Diatoms for Novel Applications in Nanotechnology. *Trends Biotechnol.* **2009**, 27, 116-127.
 31. Takanoglu, D.; Yilmaz, K.; Ozcan, Y.; Karabulut, O. Structural, Electrical and Optical Properties of Thermally Evaporated Cdse and in-doped CdSe Thin Films. *Chalcogenide Lett.* **2015**, 12, 35-42.
 32. Shahbazarab, Z.; Teimouri, A.; Chermahini, A. N.; Azadi, M. Fabrication and Characterization of Nanobiocomposite Scaffold of Zein/Chitosan/Nanohydroxyapatite Prepared by Freeze-drying Method for Bone Tissue Engineering. *Int. J. Biol. Macromol.* **2018**, 108, 1017-1027.
 33. Zhang, K.; Cheng, L.; Imazato, S.; Antonucci, J. M.; Lin, N. J.; Lin-Gibson, S.; Bai, Y.; Xu, H. H. K. Effects of Dual Antibacterial Agents MDPB and Nano-silver in Primer on Microcosm Biofilm, Cytotoxicity and Dentine Bond Properties. *J. Dent.* **2013**, 41, 464-474.
 34. Mahammad, B. P.; Barua, E.; Deb, P.; Deoghare, A. B.; Pandey, K. M. Investigation of Physico-mechanical Behavior, Permeability and Wall Shear Stress of Porous HA/PMMA Composite Bone Scaffold. *Arab. J. Sci. Eng.* **2020**, 45, 5505-5515.
 35. Li, Z.; Ramay, H. R.; Hauch, K. D.; Xiao, D.; Zhang, M. Chitosan-alginate Hybrid Scaffolds for Bone Tissue Engineering. *Biomaterials* **2005**, 26, 3919-3928.
 36. Venkatesan, J.; Bhatnagar, I.; Kim, S. Chitosan-Alginate Biocomposite Containing Fucoidan for Bone Tissue Engineering. *Mar. Drugs* **2014**, 12, 300-316.
 37. Daemi, H.; Barikani, M. Synthesis and Characterization of Calcium Alginate Nanoparticles, Sodium Homopolymannuronate Salt and Its Calcium Nanoparticles. *Sci. Iran.* **2012**, 19, 2023-2028.
 38. Yasmeen, S.; Kabiraz, M. K.; Saha, B.; Qadir, M.-D.; Gafur, M.; Masum, S. Chromium (VI) Ions Removal from Tannery Effluent using Chitosan-Microcrystalline Cellulose Composite as Adsorbent. *Int. Res. J. Pure. Appl. Chem.* **2016**, 10, 1-14.
 39. Gendron-Badou, A.; Coradin, T.; Maquet, J.; Fröhlich, F.; Livage, J. Spectroscopic Characterization of Biogenic Silica. *J. Non-Cryst. Solids* **2003**, 316, 331-337.
 40. Gélabert, A.; Pokrovsky, O. S.; Schott, J.; Boudou, A.; Feurtet-Mazel, A.; Mielczarski, J.; Mielczarski, E.; Mesmer-Dudons, N.; Spalla, O. Study of Diatoms/Aqueous Solution Interface. I. Acid-Base Equilibria and Spectroscopic Observation of Freshwater and Marine Species. *Geochim. Cosmochim. Acta* **2004**, 68, 4039-4058.
 41. Sowjanya, J. A.; Singh, J.; Mohita, T.; Sarvanan, S.; Moorthi, A.; Srinivasan, N.; Selvamurugan, N. Biocomposite Scaffolds Containing Chitosan/Alginate/Nano-silica for Bone Tissue Engineering. *Colloids Surf. B* **2013**, 109, 294-300.
 42. Manzari-Tavakoli, A.; Tarasi, R.; Sedghi, R.; Moghimi, A.; Niknejad, H. Fabrication of Nanochitosan Incorporated Polypyrrole/Alginate Conducting Scaffold for Neural Tissue Engineering. *Sci. Rep.* **2020**, 10, 22012-22021.
 43. Zhang, L.; Guo, J.; Zhou, J.; Yang, G.; Du, Y. Blend Membranes from Carboxymethylated Chitosan/Alginate in Aqueous Solution. *J. Appl. Polym. Sci.* **2000**, 77, 610-616.

Publisher's Note The Polymer Society of Korea remains neutral with regard to jurisdictional claims in published articles and institutional affiliations.